

Heavy quark drag and diffusion coefficients in the pre-hydrodynamic QCD plasma

Xiaojian Du^{1,*}

¹*Instituto Galego de Física de Altas Enerxías (IGFAE),
Universidade de Santiago de Compostela, E-15782 Galicia, Spain*

(Dated: June 6, 2023)

Kinetic and chemical equilibrations play important roles in the formation of the quark-gluon plasma (QGP) in relativistic heavy-ion collisions (HICs). These processes further influence the production of hard and electromagnetic probes in HICs, in particular, the thermalization of heavy quarks, which are produced at an extremely early time before the formation of the QGP. We calculate the drag and diffusion coefficients of heavy quarks in the pre-hydrodynamic quantum chromodynamic (QCD) plasma with the state-of-the-art QCD effective kinetic theory (EKT) solver. We present the time, momentum, and angular dependencies of these coefficients for gluon and quark contributions separately, showing the effects of isotropization and chemical equilibration from the QCD plasma. We also provide a simple formula to estimate the heavy quark energy loss within the pre-hydrodynamic plasma in both weakly and strongly coupled cases based on the attractor theory.

PACS numbers:

Introduction — Thermalization is omnipresent and there are two main categories of thermalization systems that are being widely studied due to the simplification of degrees of freedom at certain scales. One is the thermalization of many-body systems, where the microscopic dynamics of single particles can be coarse-grained and the emergent behavior is more interesting. The other one is the thermalization of open quantum systems, where the objects have distinguished degrees of freedom or scales from the background medium environment, and tracing out the environment leaves a simple dynamical description of the system in the medium. Relativistic heavy-ion collisions (HICs) are such experiments that both categories are present for us to understand the fundamental strong interaction.

The quark-gluon plasma (QGP) containing free quark and gluon degrees of freedom, as a many-body system, can only be produced in the early universe or HICs nowadays. The main period of the QGP evolution in HICs is successfully described by a near-equilibrium macroscopic theory, the relativistic hydrodynamics [1–8], in terms of the energy-momentum tensor. A more involved tool that can describe the non-equilibrium and pre-hydrodynamic QGP is the effective kinetic theory (EKT) [9], in terms of particle distributions. This theory is initially implemented as Yang-Mills kinetics [10, 11] including gluon, and developed into quantum chromodynamic (QCD) kinetics [12, 13] including both gluon and quarks. Various models as similar approaches or as simplified versions of EKT exist [14–22]. Although the pre-hydrodynamic QGP in HICs is complicated as is anisotropic and chemically out-of-equilibrium, there are still some universal descriptions of the pre-hydrodynamic QGP based on simple conservation laws, independent of the microscopic physics, such as the attractor theory [23–32].

On the other hand, heavy quarks have distinguished mass scales from light partons in the QGP, and are pro-

duced as open quantum systems due to their large mass thresholds. Heavy quark thermalization is contributed by energy loss and diffusion. Most of the heavy quarks are produced within the momentum range $p \lesssim m_{HQ}$, where the radiative energy loss can be neglected and the collisional energy loss dominates [33]. They are produced at a time scale $\tau \simeq \frac{1}{m_{HQ}}$ before the hydrodynamization of the QGP at $\tau_h \simeq \frac{4\pi\eta}{Ts}$, and relax at a much later time $\tau_R \simeq \frac{m_{HQ}}{T}\tau_h$. Thus, most of the heavy quark thermalization simulations [34–49] are focusing on the hydrodynamic stage when the QGP is nearly thermalized. There are some efforts in addressing the heavy quark thermalization in the pre-hydrodynamic glasma or QGP [50–52] taking care of the anisotropy or chemical effects. The EKT allows us to calculate the heavy quark diffusion [53] as well as jet momentum broadening [54] dynamically during the pre-hydrodynamic stage from the first principle. Furthermore, the recent developments of the EKT to a full QCD level will complete this picture.

In this letter, we will show the first-principle calculations of heavy quark drag and diffusion coefficients in the QCD plasma, from the state-of-the-art QCD effective kinetic theory (QCD EKT) solver [13] including both gluon and quark dynamics. As an add-on, with the attractor theory, we will also provide a simple formula to estimate the heavy quark energy loss within the pre-hydrodynamic QGP in both weakly and strongly coupled plasmas.

Pre-hydrodynamic QCD plasma & attractor — The QCD plasma out-of-equilibrium before the formation of the hydrodynamic state can be described by the QCD EKT, with a Bjorken expansion at the early stage of HICs. Within the EKT, the evolution of gluon and light quark/anti-quarks as constitutes of the QCD plasma is formulated as a set of coupled Boltzmann equations [55] with $a = g, q, \bar{q}$ and flavor number $N_f = 3$

$$\frac{\partial f_a(\vec{p}, \tau)}{\partial \tau} - \frac{p_{\parallel} \partial f_a(\vec{p}, \tau)}{\tau \partial p_{\parallel}} = C_a^{1 \leftrightarrow 2, 2 \leftrightarrow 2}[f](\vec{p}, \tau). \quad (1)$$

The collision integrals $C_a[f]$ contain elastic $2 \leftrightarrow 2$ processes with screening masses fitted to the Hard Thermal Loop (HTL) calculation [9], as well as collinear inelastic $1 \leftrightarrow 2$ processes including the Landau-Pomeranchuk-Migdal (LPM) effect [56–58]. Both processes are calculated with leading-order (LO) perturbative QCD (pQCD). Details of the QCD EKT and its numerical implementations can be found in our previous paper [13]. The expansion term with a factor of $1/\tau$ renders an anisotropization of the plasma in the longitudinal-transverse plane at an early time, while the collision terms $C_a[f]$ take over the evolution at a later time and drive the plasma to reach hydrodynamic equilibrium, in both kinetic and chemical sense.

The early-time expansion and the later-on hydrodynamization are independent of the details of the microscopic interactions in the kinetic theory, resulting in a universal attractor solution. This solution connects the energy density of the plasma at any time $e(\tau)$ to its initial value e_0 in a simple and universal way [27, 28]

$$\tau^{\frac{4}{3}} e(\tilde{\omega}) = \left(4\pi \frac{\eta}{s}\right)^{\frac{4}{9}} \left(\frac{\pi^2 \nu_{\text{eff}}}{30}\right)^{\frac{1}{9}} (\tau_0 e_0)^{\frac{8}{9}} C_\infty \mathcal{E}(\tilde{\omega}). \quad (2)$$

The function $\mathcal{E}(\tilde{\omega})$ is called the energy attractor in terms of the universal and dimensionless time scale $\tilde{\omega} = \frac{\tau T_s}{4\pi\eta}$. The effective temperature can be evaluated by Landau matching $T = \left(\frac{30e(\tau)}{\pi^2 \nu_{\text{eff}}}\right)^{\frac{1}{4}}$. The $N_f = 3$ massless QCD degeneracy factor $\nu_{\text{eff}} = \nu_g + \frac{7}{4}\nu_q N_f = 47.5$ and $C_\infty = 0.87$ are both constants. The shear viscosity over entropy density ratio η/s directly reflects how strong the interaction coupling is and how quick the equilibration can be. Indeed, at any $\tilde{\omega}$, there is a universal energy attractor $\mathcal{E}(\tilde{\omega})$ that characterizes the degree of thermalization, valued from $\mathcal{E}(\tilde{\omega} \rightarrow 0) = 0$ to $\mathcal{E}(\tilde{\omega} \rightarrow \infty) = 1$. One can evaluate the corresponding time at any specific $\tilde{\omega}$ as [64]

$$\tau = \left(4\pi \frac{\eta}{s}\right)^{\frac{4}{3}}_{\text{prehydro}} \left(\frac{\pi^2 \nu_{\text{eff}}}{30}\right)^{\frac{1}{3}} (\tau_0 e_0)^{-\frac{1}{3}} C_\infty^{-\frac{3}{8}} \mathcal{E}^{-\frac{3}{8}}(\tilde{\omega}) \tilde{\omega}^{\frac{3}{2}}. \quad (3)$$

This means that a more strongly coupled plasma with a smaller η/s requires a shorter time to reach a certain degree of thermalization, while a more weakly coupled plasma with a larger η/s requires a longer time. As a consequence, the universality of the attractor gives the approximate relation in the pre-hydrodynamic stage

$$\tau_{\text{strong}} \left(\frac{\eta}{s}\right)_{\text{strong}}^{-\frac{4}{3}} \simeq \tau_{\text{weak}} \left(\frac{\eta}{s}\right)_{\text{weak}}^{-\frac{4}{3}}. \quad (4)$$

Although the massless QCD effective kinetic theory is conformal, one can fix the scales by matching experimental data at the end of the QGP evolution, assuming entropy conservation in the following thermal hydrodynamic stage. In equilibrium, $\mathcal{E}(\tilde{\omega} \gg 1) = 1$ and

$sT = e + p$ at zero net-baryon density. The equation of state $e = 3p$ always holds in a conformal theory. One has

$$(\tau s)_{\text{eq}} = \frac{4}{3} \frac{(\tau^{\frac{4}{3}} e)_{\text{eq}}}{(\tau^{\frac{1}{3}} T)_{\text{eq}}} = \frac{4}{3} (\tau^{\frac{4}{3}} e)_{\text{eq}}^{\frac{3}{4}} \left(\frac{\pi^2 \nu_{\text{eff}}}{30}\right)^{\frac{1}{4}}, \quad (5)$$

and the entropy density can be related to the charged particle multiplicity via $dN_{\text{ch}}/d\eta = \frac{N_{\text{ch}}}{S_\perp} (\tau s)_{\text{eq}} S_\perp$ with $S/N_{\text{ch}} = 8.36$ [59] and S_\perp the transverse area of the collision. As a consequence, one has the following relation to constrain the scales in the initial condition $\tau_0 e_0$

$$\frac{dN_{\text{ch}}}{d\eta} = \frac{4}{3} \frac{N_{\text{ch}}}{S} \left(4\pi \frac{\eta}{s}\right)_{\text{average}}^{\frac{1}{3}} \left(\frac{\pi^2 \nu_{\text{eff}}}{30}\right)^{\frac{1}{3}} (\tau_0 e_0)^{\frac{2}{3}} C_\infty^{\frac{3}{4}} S_\perp. \quad (6)$$

Matching the LHC 5.02 TeV Pb+Pb collision data [60], $dN_{\text{ch}}/d\eta = 1942$ and $S_\perp = 138\text{fm}^2$ assuming strongly coupled plasma at the holographic bound $\eta/s = 1/4\pi$ [61] for the hydrodynamic evolution, one can determine the value of $\tau_0 e_0 = 1.961\text{GeV}^3$ in this specific collision system. One has further the rescaling formula to evaluate the initial energy density in other circumstances

$$\tau_0 e_0 = 1.961\text{GeV}^3 \left(\frac{dN_{\text{ch}}}{d\eta}\right)^{\frac{3}{2}}_{1942} \left(4\pi \frac{\eta}{s}\right)_{\text{average}}^{-\frac{1}{2}} \left(\frac{S_\perp}{138\text{fm}^2}\right)^{-\frac{3}{2}}. \quad (7)$$

The initial energy is mainly deposited by an over-occupied, anisotropic, and gluon-saturated state; and described by the CGC-inspired distribution [11, 62]

$$f_g(\vec{p}, \tau_0) = \frac{10.5}{\lambda_0} \frac{1.8Q_s}{\sqrt{p_\perp^2 + (\xi p_\parallel)^2}} \exp\left[-\frac{2}{3} \frac{p_\perp^2 + (\xi p_\parallel)^2}{(1.8Q_s)^2}\right],$$

$$f_q(\vec{p}, \tau_0) = f_{\bar{q}}(\vec{p}, \tau_0) = 0, \quad (8)$$

with the momentum decomposition in transverse and longitudinal directions $\vec{p} = (\vec{p}_\perp, p_\parallel)$. The anisotropic parameter is typically chosen as $\xi = 10$. A typical value for the 'tHooft coupling $\lambda_0 = g_0^2 N_c$ chosen in simulating weakly coupled gauge field in CGC effective theory is $\lambda_0 = 10$, which is at least reasonable as well at the initial time for our QCD kinetic simulation when the system has a high temperature. The general 'tHooft coupling $\lambda = g^2 N_c$ entering into the QCD kinetic simulation is controlling the thermalization speed, which can be further reflected in the macroscopic coefficient η/s . Although a realistic QCD running coupling requires the coupling λ to increase (resulting in a decreasing value of η/s) at a lower energy scale which happens at the later stage of the hydrodynamization, the massless QCD is scale-invariant. We keep the coupling $\lambda = 10$ throughout the QCD kinetic simulation and perform rescaling of physical quantities to evaluate strongly coupled plasma, where the validity of both the kinetic theory and the perturbation theory breaks down. General rescaling can be achieved due to the universality of the attractor solutions, from the basic

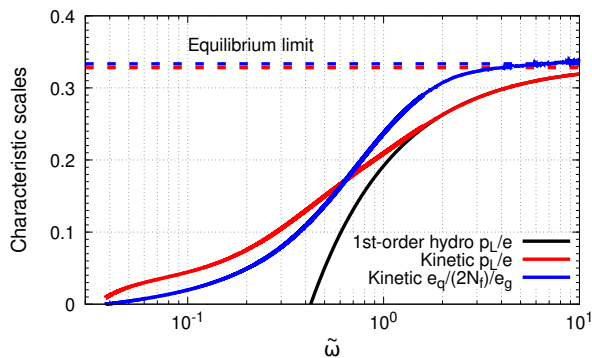


FIG. 1: Typical characteristic scales of isotropization p_L/e (red) and chemical equilibration e_q/e_g (blue) in terms of universal time $\tilde{\omega}$, compared to the hydrodynamic limit (black) and their equilibrium limits (dashed).

principles of energy conservation and conformality, regardless of the coupling or modeling. The initial time for the QCD kinetic evolution is approximately the inverse of the saturation scale for the gauge fields $\tau_0 \simeq 1/Q_s$ before the formation of the quasi-particles in the kinetic theory picture. Without losing generality, by choosing $\tau_0 = Q_s^{-1}$ we can calculate the initial energy density and one gets $\tau_0 e_0 = 0.5858 Q_s^3 = 1.961 \text{ GeV}^3$. Now one can estimate that $Q_s = 1.496 \text{ GeV}$ and $\tau_0 = Q_s^{-1} = 0.134 \text{ fm}$, smaller than the typical hydrodynamization time $\tau_h \simeq 0.2 - 0.6 \text{ fm}$ but at the same order of magnitude.

By solving the QCD kinetic theory, one gets the time evolution of the distributions $f_g(\vec{p}, \tau)$, $f_q(\vec{p}, \tau)$, $f_{\bar{q}}(\vec{p}, \tau)$. There are certain quantities that one can calculate to characterize the equilibration of the QCD plasma, such as the energy-momentum tensor

$$T^{\mu\nu} = \int \frac{d^3p}{(2\pi)^3} \frac{p^\mu p^\nu}{p} \{ \nu_g f_g(\vec{p}) + \nu_q N_f [f_q(\vec{p}) + f_{\bar{q}}(\vec{p})] \}. \quad (9)$$

The longitudinal pressure over energy density ratio $p_L/e = T^{zz}/T^{\tau\tau}$ characterizes the isotropization of the plasma with an equilibrium limit of $1/3$. The quark over gluon energy density ratio e_q/e_g characterizes the chemical equilibration of the plasma with an equilibrium limit $(7\nu_q N_f)/(4\nu_g)$. We show these characteristic scales in Fig. 1 in terms of the universal time scale $\tilde{\omega}$ for the QCD plasma. The anisotropy of the plasma approaches the hydrodynamic limit at around $\tilde{\omega} \simeq 1 - 2$ while its equilibrium limit has to be reached after a much longer time. The chemical equilibration roughly finishes later than $\tilde{\omega} \simeq 2 - 3$ where the quark over gluon density ratio tends to be a plateau.

The non-equilibrium gluon, quark/antiquark distributions in the QCD plasma from the initial time $\tau_0 \simeq 1/Q_s$ to the hydrodynamization time τ_h ($\omega \simeq 1 - 2$) serve as the background for heavy quarks to lose energy and diffuse, even before the formation of the hydrodynamic plasma. These non-equilibrium distributions will deviate

the transport coefficients of heavy quarks from thermal cases, and open an opportunity to extend heavy quark simulations to the pre-hydrodynamic stage of HICs.

Heavy quark thermalization — The heavy quark thermalization with soft collisions from the background QCD plasma can be described by a stochastic differential equation (SDE) in phase space (\vec{x}, \vec{p}) , the Langevin equation

$$\begin{aligned} dx_i &= \frac{p_i}{E(\vec{p})} d\tau, \\ dp_i &= -A_i(\vec{p}, \tau) d\tau + \sigma_{ij}(\vec{p}, \tau) dW_j, \end{aligned} \quad (10)$$

with a Wiener process $dW_j \sim \mathcal{N}(0, d\tau)$ correlated as $\langle dW_i dW_j \rangle = \delta_{ij} d\tau$. Applying Ito's lemma to Eq. (10) up to order $\mathcal{O}(d\tau)$, the corresponding Fokker-Planck equation with diffusion coefficients $B_{ij}(\vec{p}, \tau) = \frac{1}{2} \sigma_{ik} \sigma_{jk}$ reads

$$\frac{\partial f_Q(\vec{p}, \tau)}{\partial \tau} = \frac{\partial [A_i(\vec{p}, \tau) f_Q(\vec{p}, \tau)]}{\partial p_i} + \frac{\partial^2 [B_{ij}(\vec{p}, \tau) f_Q(\vec{p}, \tau)]}{\partial p_i \partial p_j} \quad (11)$$

Notice that both drag coefficients $A_i(\vec{p}, \tau)$ and diffusion coefficients $B_{ij}(\vec{p}, \tau)$ depend not only on the heavy quark momentum \vec{p} but also on the time of the evolving pre-hydrodynamics QCD plasma τ . There are two evolving chemical contributions, from gluon collisions $gQ \rightarrow gQ$ and from quark/antiquark collisions $qQ \rightarrow qQ$ (including the factor $2N_f$ in the quark sector)

$$\begin{aligned} A_i(\vec{p}, \tau) &= A_{g,i}(\vec{p}, \tau) + A_{q,i}(\vec{p}, \tau), \\ B_{ij}(\vec{p}, \tau) &= B_{g,ij}(\vec{p}, \tau) + B_{q,ij}(\vec{p}, \tau). \end{aligned} \quad (12)$$

The drag and diffusion coefficients for heavy quark Q collided by a parton $a = g, q, \bar{q}$ in the QCD plasma can be calculated as [34]

$$\begin{aligned} A_{a,i}(\vec{p}, \tau) &= \frac{1}{2E(\vec{p})} \int d\Pi \overline{|M_{aQ \rightarrow aQ}|^2} \nu_a f_a(\vec{p}_a, \tau) \\ &\times (1 \pm f_a(\vec{p}'_a, \tau)) (1 - f_Q(\vec{p}', \tau)) (\vec{p} - \vec{p}')_i, \\ B_{a,ij}(\vec{p}, \tau) &= \frac{1}{4E(\vec{p})} \int d\Pi \overline{|M_{aQ \rightarrow aQ}|^2} \nu_a f_a(\vec{p}_a, \tau) \\ &\times (1 \pm f_a(\vec{p}'_a, \tau)) (1 - f_Q(\vec{p}', \tau)) (\vec{p} - \vec{p}')_i (\vec{p} - \vec{p}')_j, \end{aligned}$$

with

$$\begin{aligned} d\Pi &= \frac{d^3 p_a}{(2\pi)^3 2E_a(\vec{p}_a)} \frac{d^3 p'_a}{(2\pi)^3 2E'_a(\vec{p}'_a)} \frac{d^3 p'_Q}{(2\pi)^3 2E'(\vec{p}')} \\ &\times (2\pi)^4 \delta^{(4)}(P + P_a - P' - P'_a). \end{aligned} \quad (13)$$

Due to the small occupation of heavy quarks $f_Q(\vec{p}', \tau) \ll 1$, the Fermi-blocking factor for the heavy quark can be neglected. We calculate the amplitude squares $\overline{|M_{aQ \rightarrow aQ}|^2}$ in the LO pQCD, and further implement the dynamical screening mass m_D^2 [65].

The relations between $A_{a,i}$ and $B_{a,ij}$ are complicated in the anisotropic plasma [66]. To calculate the drag and diffusion coefficients, we assume a charm quark mass $m_c = 1.5 \text{ GeV}$, and the coupling in the collisional amplitude squares the same as the background QCD plasma $\alpha_s = \frac{g^2}{4\pi} = \frac{\lambda}{4\pi N_c}$ with $\lambda = 10$.

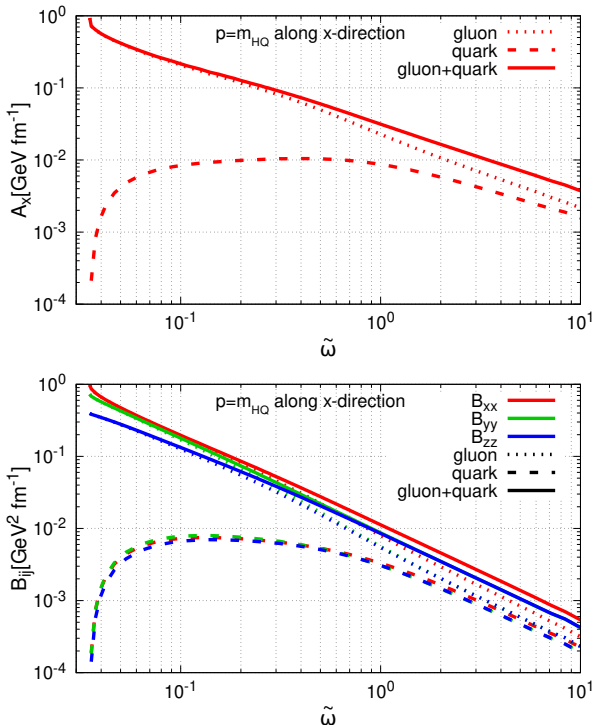


FIG. 2: Drag and diffusion coefficients $A_x(\tilde{\omega})$, $B_{xx}(\tilde{\omega})$ (red), $B_{yy}(\tilde{\omega})$ (green), $B_{zz}(\tilde{\omega})$ (blue) for gluon and quark (with factor $2N_f$), as a function of universal time $\tilde{\omega}$, with heavy quark momentum $p=1.5$ GeV and mass $m_{HQ} = 1.5$ GeV. Gluon and quarks are plotted as dotted and dashed curves respectively.

Heavy quark drag and diffusion coefficients — At mid-rapidity in HICs, one expects a longitudinally boost invariant plasma, and usually cares only about the heavy quark evolution in the transverse plane. Without loss of generality, we choose the momentum direction of the heavy quark in the transverse plane, to be along the x-axis, the perpendicular direction in the transverse plane to be along the y-axis, and the longitudinal direction along the z-axis. So we choose $\vec{p} = (p_x, p_y, p_z) = (p, 0, 0)$ in Cartesian coordinate or $\vec{p} = (p, \cos(\theta), \phi) = (p, 0, 0)$ in cylindrical coordinate if not stated otherwise. By default, $\vec{p} = (p, 0, 0)$, the symmetry of the integration will give trivial values of A_y , A_z , as well as off-diagonal terms in the B_{ij} matrix, even if the plasma is anisotropic.

We plot the time evolution of coefficients A_x , B_{xx} , B_{yy} , B_{zz} in Fig. 2 including their gluon and quark components. The time evolution of the coefficients in terms of $\tilde{\omega}$ roughly features a power-law behavior. One sees the isotropization more clearly in the lower panel of Fig. 2, that B_{yy} is deviated from B_{zz} at an early time and is approaching B_{zz} at a late time. The increasing trend in quark contribution is clearly shown in both panels, that the drag and diffusion coefficients contributed by quarks become comparable to gluon at a late time. However, due to the Bose-enhancement and Fermi-blocking factors, the

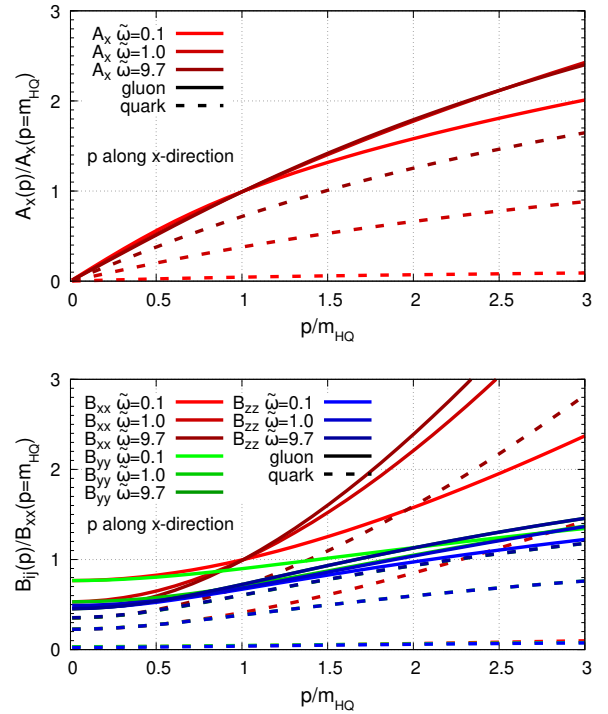


FIG. 3: Drag and diffusion coefficients $A_x(\vec{p})$, $B_{xx}(\vec{p})$ (red), $B_{yy}(\vec{p})$ (green), $B_{zz}(\vec{p})$ (blue) for gluon and quark (with factor $2N_f$), as a function of rescaled momentum p/m_{HQ} . Coefficients are normalized by either $A_x(p = m_{HQ})$ or $B_{xx}(p = m_{HQ})$. The early time coefficients are in lighter colors and the late time coefficients are in darker colors.

quark contribution in the coefficients is not as significant as it is in the energy density of the QCD plasma as we see in Fig. 1, where $e_q \simeq 2e_g$ at the later time.

The momentum dependencies of the coefficients are shown in Fig. 3 for various times, where we have normalized everything by either $A_x(p = m_{HQ})$ or $B_{xx}(p = m_{HQ})$ so that these two coefficients are fixed at the point $(p/m_{HQ} = 1, 1)$. By performing this normalization, one finds a universality of $A_x(p)$ at a different time for small momentum $p \leq m_{HQ}$, and the dependence becomes linear at the late stage. Isotropization can also be found in the lower panel that $B_{yy}(p)$ gradually approaches $B_{zz}(p)$ at a later time. $B_{yy}(p)$ is the same as B_{xx} for $p \ll m_{HQ}$ for all time, the reason is obvious. The increasing trend of the quark contribution is also presented.

Now we release our constraints for the heavy quark momentum to be in the transverse plane only. Still, look at the typical momentum $p = m_{HQ}$, but in the x-z plane, we present the coefficients as a function of the $\cos(\theta) = p_z/p$ in Fig. 4. Now the breaking symmetries in the integrals result in many more nontrivial coefficients A_x , A_z , B_{xx} , B_{xz} , B_{yy} , B_{zz} but they have vanishing points at certain angles. For example, at $\cos(\theta) = 0$, the heavy quark momentum is in the transverse plane and A_z vanishes; while at $\cos(\theta) = \pm 1$, the heavy quark momentum is in

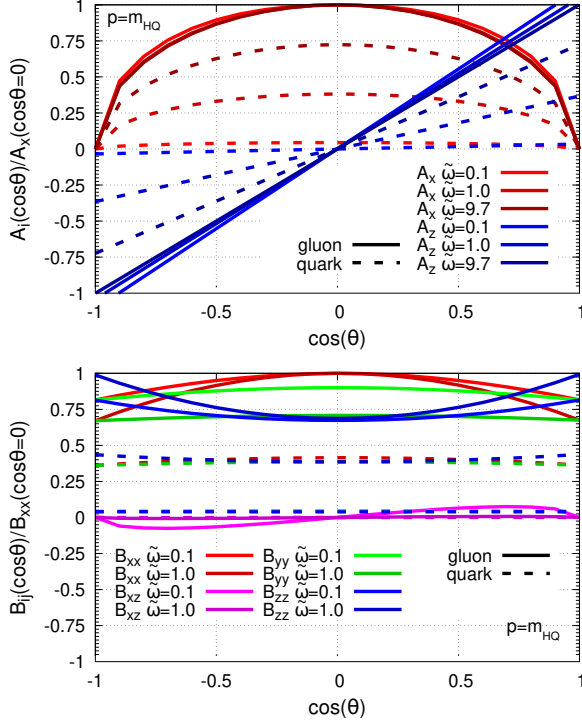


FIG. 4: Drag and diffusion coefficients $A_i(\vec{p}, \tilde{\omega})$, $B_{ij}(\vec{p}, \tilde{\omega})$ for gluon and quark (with factor $2N_f$), as a function of angle $\cos(\theta)$ in x-z plane, normalized by values of A_x and B_{xx} when $\cos(\theta) = 0$.

the longitudinal plane, and A_x vanishes.

Phenomenological consequences — With the weakly coupled plasma simulated from the kinetic theory and the universality of attractor theory, we can estimate the energy loss of heavy quarks in a strongly coupled pre-hydrodynamic QCD plasma. Indeed, for any time convolution of a physical quantity $\mathcal{C}(\tau)$

$$\int_{\tau_0}^{\tau_h} \mathcal{C}(\tau) d\tau_{\text{strong}} \simeq \int_{\tau_0}^{\tau^*} \mathcal{C}(\tau) d\tau_{\text{weak}} \frac{(\eta/s)_{\text{strong}}^{\frac{4}{3}}}{(\eta/s)_{\text{weak}}^{\frac{4}{3}}}, \quad (14)$$

where we have to fix the same initial time τ_0 since the early time plasma is weakly coupled, until a hydrodynamization time τ_h in a strongly coupled plasma when $\tilde{\omega} \simeq 1 - 2$. With attractor theory, one can estimate the hydrodynamization time in strongly coupled plasma τ_h from the time one calculated from weakly coupled plasma τ^* when $\tilde{\omega} \simeq 1 - 2$. Then the time convolution in Eq. (14) can be simply evaluated in the weakly coupled plasma where we already have all the information. For the weakly coupled plasma $\lambda = 10$ we have calculated, one has $(\eta/s)_{\text{weak}} = 1$ and $\tau^* \simeq 100 - 275Q_s^{-1}$ according to the coupling independent universal time $\tilde{\omega} \simeq 1 - 2$.

Strongly coupled plasma also gives a larger value of the coefficients, the drag and diffusion coefficients are roughly scaled as $\mathcal{C}(\lambda) \simeq \left(\frac{\lambda}{10}\right)^2 \mathcal{C}(\lambda = 10)$. Now, one can

evaluate the energy loss and diffusion of heavy quarks as

$$\left\langle \frac{\Delta p_i}{p_0} \right\rangle_{\text{loss}} \simeq \int_{\tau_0}^{\tau^*} -\frac{A_i(\vec{p}, \tau)}{p_0} d\tau \left(\frac{\eta}{s}\right)^{\frac{4}{3}} \left(\frac{\lambda}{10}\right)^2 \quad (15)$$

$$\left\langle \frac{\Delta p_i \Delta p_j}{p_0^2} \right\rangle_{\text{diff}} \simeq \int_{\tau_0}^{\tau^*} \frac{B_{ij}(\vec{p}, \tau)}{p_0^2} \delta_{ij} d\tau \left(\frac{\eta}{s}\right)^{\frac{4}{3}} \left(\frac{\lambda}{10}\right)^2 \quad (16)$$

Focusing on the transverse plane and assuming the heavy quark initial momentum to be $p_0 \leq m_{HQ}$ in the x-direction, one has roughly a linear momentum dependence on the drag coefficient $A_x(\vec{p}, \tau) \simeq \frac{A_x(m_{HQ}, \tau)}{m_{HQ}} p_x$, so the energy loss is independent of the initial momentum. Solving Eq. (15), one has (see the supplemental material)

$$\left\langle \frac{\Delta p_x}{p_0} \right\rangle_{\text{loss}} \simeq 1 - e^{-\int_{\tau_0}^{\tau^*} \frac{A_x(m_{HQ}, \tau)}{m_{HQ}} d\tau \left(\frac{\eta}{s}\right)^{\frac{4}{3}} \left(\frac{\lambda}{10}\right)^2}. \quad (17)$$

Numerical evaluations for τ^* corresponding to $\tilde{\omega} = 1$ and $\tilde{\omega} = 2$ give $\left\langle \frac{\Delta p}{p_0} \right\rangle_{\text{loss}} \simeq 1 - e^{-0.56 \left(\frac{\eta}{s}\right)^{\frac{4}{3}} \left(\frac{\lambda}{10}\right)^2}$ up to $\tilde{\omega} = 1$, and $\left\langle \frac{\Delta p}{p_0} \right\rangle_{\text{loss}} \simeq 1 - e^{-0.89 \left(\frac{\eta}{s}\right)^{\frac{4}{3}} \left(\frac{\lambda}{10}\right)^2}$ up to $\tilde{\omega} = 2$. Before the plasma reaches the hydrodynamic stage, it could be neither so weakly coupled nor that strongly coupled, and one may simply estimate the value with different η/s and λ accordingly.

Conclusions & Outlook — In this letter, we calculate the heavy quark drag and diffusion coefficients in a weakly coupled pre-hydrodynamic QCD plasma from a first principle and the state-of-art QCD EKT solver. We present the time, momentum, and angular dependencies of the coefficients A_i , B_{ij} with all indices. With arguments from the attractor theory, we provide a simple formula to evaluate the heavy quark energy loss even in a strongly coupled pre-hydrodynamic plasma. For complete calculations on heavy quark energy loss in the pre-hydrodynamic stage, one needs to solve for the time evolution of the QCD plasma with evolving coupling in full phase space and calculate all the drag and diffusion coefficients in all momenta and angles as functions of time $A_i(\vec{p}, \tau)$, $B_{ij}(\vec{p}, \tau)$. Then one can simulate heavy quarks in this dynamically evolving plasma via kinetic equations in Eq. (10) or Eq. (11), which is out of the scope of the current work, and we leave that to a future study.

Acknowledgement — The author thanks Kirill Boguslavski, Florian Lindenbauer, Meijian Li, and Bin Wu for helpful discussions. The author is supported by Xunta de Galicia (Centro singular de investigacion de Galicia accreditation 2019-2022), European Union ERDF, the “Maria de Maeztu” Units of Excellence program under project CEX2020-001035-M, the Spanish Research State Agency under project PID2020-119632GB-I00, and European Research Council under project ERC-2018-ADG-835105 YoctoLHC. The author also acknowledges the computational resources supported by LUMI-C super-computer, under The European High Performance Computing Joint Undertaking grant EHPC-REG-2022R03-192 Non-equilibrium Quark-Gluon Plasma.

SUPPLEMENTAL MATERIAL

Below, we show how to estimate the energy loss according to scaling and derive Eq. (17). Since $A_x(\vec{p}, \tau) \simeq \frac{A_x(m_{\text{HQ}}, \tau)}{m_{\text{HQ}}} p_x$ for $p_x \leq m_{\text{HQ}}$, one has

$$\left\langle \frac{dp_x}{p_0} \right\rangle_{\text{loss}} = -\frac{A_x(\vec{p}, \tau)}{p_0} d\tau \left(\frac{\eta}{s}\right)^{\frac{4}{3}} \left(\frac{\lambda}{10}\right)^2 \quad (18)$$

$$\simeq -\frac{A_x(m_{\text{HQ}}, \tau)}{m_{\text{HQ}}} \frac{p_x}{p_0} d\tau \left(\frac{\eta}{s}\right)^{\frac{4}{3}} \left(\frac{\lambda}{10}\right)^2 \quad (19)$$

and the time convolution gives

$$-\int_{\tau_0}^{\tau^*} \frac{A_x(m_{\text{HQ}}, \tau)}{m_{\text{HQ}}} d\tau \left(\frac{\eta}{s}\right)^{\frac{4}{3}} \left(\frac{\lambda}{10}\right)^2 \quad (20)$$

$$\simeq \int_{p_0}^{p_0 - \Delta p_x} \left\langle \frac{dp_x}{p_x} \right\rangle_{\text{loss}} = \ln \left(1 - \left\langle \frac{\Delta p_x}{p_0} \right\rangle_{\text{loss}} \right),$$

we arrive at

$$\left\langle \frac{\Delta p_x}{p_0} \right\rangle_{\text{loss}} \simeq 1 - e^{-\int_{\tau_0}^{\tau^*} \frac{A_x(m_{\text{HQ}}, \tau)}{m_{\text{HQ}}} d\tau \left(\frac{\eta}{s}\right)^{\frac{4}{3}} \left(\frac{\lambda}{10}\right)^2}. \quad (21)$$

* Electronic address: xiaojian.du@usc.es

- [1] I. Muller, Z. Phys. **198**, 329 (1967).
- [2] W. Israel and J. M. Stewart, Annals Phys. **118**, 341 (1979).
- [3] R. Baier, P. Romatschke, D. T. Son, A. O. Starinets, and M. A. Stephanov, JHEP **04**, 100 (2008), 0712.2451.
- [4] M. Luzum and P. Romatschke, Phys. Rev. C **78**, 034915 (2008), [Erratum: Phys.Rev.C 79, 039903 (2009)], 0804.4015.
- [5] B. Schenke, S. Jeon, and C. Gale, Phys. Rev. Lett. **106**, 042301 (2011), 1009.3244.
- [6] H. Song, S. A. Bass, U. Heinz, T. Hirano, and C. Shen, Phys. Rev. Lett. **106**, 192301 (2011), [Erratum: Phys.Rev.Lett. 109, 139904 (2012)], 1011.2783.
- [7] L. Pang, Q. Wang, and X.-N. Wang, Phys. Rev. C **86**, 024911 (2012), 1205.5019.
- [8] L. Du and U. Heinz, Comput. Phys. Commun. **251**, 107090 (2020), 1906.11181.
- [9] P. B. Arnold, G. D. Moore, and L. G. Yaffe, JHEP **01**, 030 (2003), hep-ph/0209353.
- [10] A. Kurkela and E. Lu, Phys. Rev. Lett. **113**, 182301 (2014), 1405.6318.
- [11] A. Kurkela and Y. Zhu, Phys. Rev. Lett. **115**, 182301 (2015), 1506.06647.
- [12] A. Kurkela and A. Mazeliauskas, Phys. Rev. D **99**, 054018 (2019), 1811.03068.
- [13] X. Du and S. Schlichting, Phys. Rev. D **104**, 054011 (2021), 2012.09079.
- [14] P. Romatschke and M. Strickland, Phys. Rev. D **68**, 036004 (2003), hep-ph/0304092.
- [15] Z. Xu and C. Greiner, Phys. Rev. C **71**, 064901 (2005), hep-ph/0406278.
- [16] M. Martinez and M. Strickland, Nucl. Phys. A **848**, 183 (2010), 1007.0889.
- [17] J.-P. Blaizot, J. Liao, and L. McLerran, Nucl. Phys. A **920**, 58 (2013), 1305.2119.
- [18] S. Kamata, M. Martinez, P. Plaschke, S. Ochsenfeld, and S. Schlichting, Phys. Rev. D **102**, 056003 (2020), 2004.06751.
- [19] A. Behtash, S. Kamata, M. Martinez, T. Schäfer, and V. Skokov, Phys. Rev. D **103**, 056010 (2021), 2011.08235.
- [20] V. E. Ambrus, S. Schlichting, and C. Werthmann, Phys. Rev. Lett. **130**, 152301 (2023), 2211.14356.
- [21] S. Barrera Cabodevila, C. A. Salgado, and B. Wu, Phys. Lett. B **834**, 137491 (2022), 2206.12376.
- [22] J. Brewer, W. Ke, L. Yan, and Y. Yin (2022), 2212.00820.
- [23] M. P. Heller and M. Spalinski, Phys. Rev. Lett. **115**, 072501 (2015), 1503.07514.
- [24] P. Romatschke, Phys. Rev. Lett. **120**, 012301 (2018), 1704.08699.
- [25] M. Strickland, JHEP **12**, 128 (2018), 1809.01200.
- [26] A. Kurkela, W. van der Schee, U. A. Wiedemann, and B. Wu, Phys. Rev. Lett. **124**, 102301 (2020), 1907.08101.
- [27] G. Giacalone, A. Mazeliauskas, and S. Schlichting, Phys. Rev. Lett. **123**, 262301 (2019), 1908.02866.
- [28] X. Du and S. Schlichting, Phys. Rev. Lett. **127**, 122301 (2021), 2012.09068.
- [29] M. P. Heller, R. Jefferson, M. Spaliński, and V. Svensson, Phys. Rev. Lett. **125**, 132301 (2020), 2003.07368.
- [30] D. Almaalol, A. Kurkela, and M. Strickland, Phys. Rev. Lett. **125**, 122302 (2020), 2004.05195.
- [31] C. Chattopadhyay, S. Jaiswal, L. Du, U. Heinz, and S. Pal, Phys. Lett. B **824**, 136820 (2022), 2107.05500.
- [32] X. Du, M. P. Heller, S. Schlichting, and V. Svensson, Phys. Rev. D **106**, 014016 (2022), 2203.16549.
- [33] G. D. Moore and D. Teaney, Phys. Rev. C **71**, 064904 (2005), hep-ph/0412346.
- [34] B. Svetitsky, Phys. Rev. D **37**, 2484 (1988).
- [35] M. Golam Mustafa, D. Pal, and D. Kumar Srivastava, Phys. Rev. C **57**, 889 (1998), [Erratum: Phys.Rev.C 57, 3499–3499 (1998)], nucl-th/9706001.
- [36] H. van Hees and R. Rapp, Phys. Rev. C **71**, 034907 (2005), nucl-th/0412015.
- [37] F. Riek and R. Rapp, Phys. Rev. C **82**, 035201 (2010), 1005.0769.
- [38] S. Cao and S. A. Bass, Phys. Rev. C **84**, 064902 (2011), 1108.5101.
- [39] M. He, R. J. Fries, and R. Rapp, Phys. Rev. C **86**, 014903 (2012), 1106.6006.
- [40] T. Lang, H. van Hees, J. Steinheimer, G. Inghirami, and M. Bleicher, Phys. Rev. C **93**, 014901 (2016), 1211.6912.
- [41] S. K. Das, F. Scardina, S. Plumari, and V. Greco, Phys. Rev. C **90**, 044901 (2014), 1312.6857.
- [42] J. Aichelin, P. B. Gossiaux, and T. Gousset, Phys. Rev. D **89**, 074018 (2014), 1307.5270.
- [43] A. Beraudo, A. De Pace, M. Monteno, M. Nardi, and F. Prino, Eur. Phys. J. C **75**, 121 (2015), 1410.6082.
- [44] T. Song, H. Berrehrah, D. Cabrera, J. M. Torres-Rincon, L. Tološ, W. Cassing, and E. Bratkovskaya, Phys. Rev. C **92**, 014910 (2015), 1503.03039.
- [45] S. Cao, T. Luo, G.-Y. Qin, and X.-N. Wang, Phys. Rev. C **94**, 014909 (2016), 1605.06447.
- [46] Z.-B. Kang, F. Ringer, and I. Vitev, JHEP **03**, 146 (2017), 1610.02043.
- [47] W. Ke, Y. Xu, and S. A. Bass, Phys. Rev. C **98**, 064901 (2018), 1806.08848.
- [48] M. He, H. van Hees, and R. Rapp, Prog. Part. Nucl. Phys. **130**, 104020 (2023), 2204.09299.

- [49] X. Du and R. Rapp, Phys. Lett. B **834**, 137414 (2022), 2207.00065.
- [50] P. Romatschke and M. Strickland, Phys. Rev. D **71**, 125008 (2005), hep-ph/0408275.
- [51] A. M. Adare, M. P. McCumber, J. L. Nagle, and P. Romatschke, Phys. Rev. C **90**, 024911 (2014), 1307.2188.
- [52] Y. Sun, G. Coci, S. K. Das, S. Plumari, M. Ruggieri, and V. Greco, Phys. Lett. B **798**, 134933 (2019), 1902.06254.
- [53] K. Boguslavski, A. Kurkela, T. Lappi, F. Lindenbauer, and J. Peuron (2023), 2303.12520.
- [54] K. Boguslavski, A. Kurkela, T. Lappi, F. Lindenbauer, and J. Peuron (2023), 2303.12595.
- [55] A. H. Mueller, Phys. Lett. B **475**, 220 (2000), hep-ph/9909388.
- [56] L. D. Landau and I. Pomeranchuk, Dokl. Akad. Nauk Ser. Fiz. **92**, 735 (1953).
- [57] L. D. Landau and I. Pomeranchuk, Dokl. Akad. Nauk Ser. Fiz. **92**, 535 (1953).
- [58] A. B. Migdal, Phys. Rev. **103**, 1811 (1956).
- [59] P. Hanus, A. Mazeliauskas, and K. Reygers, Phys. Rev. C **100**, 064903 (2019), 1908.02792.
- [60] J. Adam et al. (ALICE), Phys. Rev. Lett. **116**, 222302 (2016), 1512.06104.
- [61] P. Kovtun, D. T. Son, and A. O. Starinets, Phys. Rev. Lett. **94**, 111601 (2005), hep-th/0405231.
- [62] T. Lappi, Phys. Lett. B **703**, 325 (2011), 1105.5511.
- [63] M. He, H. van Hees, P. B. Gossiaux, R. J. Fries, and R. Rapp, Phys. Rev. E **88**, 032138 (2013), 1305.1425.
- [64] Do not be confused by the different $\tau - \eta/s$ scaling in our previous work [28] where the η/s is the average η/s of the whole QGP period dominated by the hydrodynamic stage (the same as the average η/s we use in Eq. (6)). Here we consider the η/s to be the average η/s in the pre-hydrodynamic stage (where hydrodynamics should not apply since the plasma could be highly off-thermal. This η/s reflects how fast the thermalization is, not the degree of thermalization, so it is a valid quantity), which is a short period of time among the whole QGP evolution. However, this is what we are interested in if we want to evaluate heavy quark thermalization in the pre-hydrodynamic stage, regardless of a strongly or a weakly coupled plasma.
- [65] The dynamical screening mass m_D^2 in the amplitude square is calculated from the QCD EKT, $m_D^2(\tau) = \frac{4\lambda}{N_c d_A} \int \frac{d^3 p}{p(2\pi)^3} [\nu_g C_A f_g(\vec{p}, \tau) + \nu_q C_F N_f (f_q(\vec{p}, \tau) + f_{\bar{q}}(\vec{p}, \tau))]$ to t-channel $t \rightarrow t [1 + \xi_g^2 m_D^2 / (\vec{p}_Q - \vec{p}'_Q)^2]$. The coefficient $\xi_g = 2^{-3/2} e^{5/6}$ is from fitting to the HTL results, as also described in details in our previous work [13].
- [66] In the special case of an isotropic plasma $f_a(\vec{p}) = f_a(|\vec{p}|)$, one has the tensor decomposition for the coefficients $A_i(\vec{p}, \tau) = p_i A(|\vec{p}|, \tau)$ and $\sigma_{ij}(\vec{p}, \tau) = \left(\delta_{ij} - \frac{p_i p_j}{p^2}\right) \sqrt{2B_0(|\vec{p}|, \tau)} + \frac{p_i p_j}{p^2} \sqrt{2B_1(|\vec{p}|, \tau)}$, so that the diffusion coefficients $B_{ij}(\vec{p}, \tau) = \frac{1}{2} \sigma_{ik} \sigma_{jk} = \left(\delta_{ij} - \frac{p_i p_j}{p^2}\right) B_0(|\vec{p}|, \tau) + \frac{p_i p_j}{p^2} B_1(|\vec{p}|, \tau)$. The heavy quark thermalization with expected thermal Boltzmann distribution $f_Q(\vec{p}) = \exp(-\beta E(\vec{p}))$ requires the following Einstein relation $A_{a,i} = \frac{\partial B_{a,ij}}{\partial p_j} - \beta \frac{B_{a,ij} p_j}{E(\vec{p})}$. See more discussion in [63]. However, the momentum dependencies of and the relations between $A_{a,i}$ and $B_{a,ij}$ are more complicated in an anisotropic plasma.